# FT-IR, FT-Raman, NMR spectra, and molecular structure investigation of 2,3-dibromo-N-methylmaleimide: A combined experimental and theoretical study

Mehmet Karabacak [a,*], Ali Çoruh [b], Mustafa Kurt [c]

[a] Department of Physics, Afyon Kocatepe University, 03040 Afyonkarahisar, Turkey
[b] Department of Physics, Sakarya University, Sakarya, Turkey
[c] Department of Physics, Ahi Evran University, 40100 Kırşehir, Turkey

## ARTICLE INFO

## ABSTRACT

In the present work, the experimental and theoretical vibrational spectra and chemical shifts of 2,3-dibromo-N-methylmaleimide (2,3DBrNMM, $C_5H_3NO_2Br_2$) were studied. FT-IR and FT-Raman spectra of 2,3DBrNMM in the solid phase were recorded in the region 4000–4400 $cm^{-1}$ and 3500–3550 $cm^{-1}$, respectively. The structural and spectroscopic data of the molecule in the ground state were calculated by using Hartree-Fock and density functional method (B3LYP) with the 6-31G(d), 6-31G(d,p), 6-31+G(d,p), 6-31++G(d,p), 6-311G(d), 6-311G(d,p), 6-311+G(d,p) and 6-311++G(d,p) basis sets. The scaled values have been compared with experimental FT-IR and FT-Raman spectra. The observed and calculated frequencies are found to be in good agreement. The complete assignments were performed on the basis of the total energy distribution (TED) of the vibrational modes, calculated with scaled quantum mechanics (SQM) method. $^{13}$C NMR, $^{1}$H NMR and DEPT spectra were recorded. $^{13}$C NMR and $^{1}$H NMR chemical shifts were calculated by using HF and B3LYP methods with 6-311++G(d,p) basis sets. The optimized geometric parameters (bond lengths and bond angles) were given corresponding experimental values of maleimide and 3-benzoylmethyl-2-chloro-N-methylmaleimide molecules.

© 2008 Published by Elsevier B.V.

## 1. Introduction

Derivatives of maleimide have been the subject of investigation for many reasons. The maleimide group is used in many areas such as antibiotic antitumor medicine [1] and biochemical conjugations rings [2]. N-Phenylmaleimide serves as an excellent model compound for the important class of resin/fibre advanced materials based on bismaleimides [3–5]. Example of the compound N-methylmaleimide is especially preferred from the standpoints of heat resistance, mechanical properties, and transparency.

Because of their spectroscopic properties and chemical significance in particular, maleimide and its derivatives have been studied extensively by spectroscopic (IR and Raman spectra) and theoretical methods. Vibrational modes and frequency analyses have been assigned in extensive recent studies on vibrational spectra of substituted maleimides [3,4,6–8]. Lazslo et al. [8] investigated the molecular structure of maleimide by using electron diffraction experimental method and MINDO/3 and CNDO/2 calculation methods. They determined bond lengths and angles of maleimide and related molecules. Harsányi et al. [7] studied all

vibrations of maleimide experimental and theoretical. Parker studied extensively the vibrational assignments of infrared (IR), Fourier transform Raman (FT-Raman) and inelastic neutron scattering of N-methylmaleimide [3]. N-Phenylmaleimide and N-(perdeuterophenyl)maleimide are investigated experimentally (infrared, Raman and inelastic neutron scattering (INS) spectroscopies) and theoretically with density functional theory (DFT) [4]. The infrared and Raman spectra of N-methylmaleimide (solid, solution, gas) and of ($\pi$-N-methylmaleimide) iron tetracarbonyl (solid, solution) which the assignment of the normal modes of both molecules was offered and compared with the data for ($\pi$-maleic anhydride) iron tetracarbonyl are obtained by Lokshin et al. [6]. Steege and Buma [9] investigated the spectroscopic and dynamic properties of the strongly one–photon absorbing $S4(\pi C=C\pi^*)$ state of maleimide and N-methylmaleimide with an experimental approach that combined with ab initio calculations of the electronic structure of the molecules. N-Phenylmaleimide and N-ethylmaleimide are also studied by X-ray crystallography [10–11].

Literature survey reveals that to the best of our knowledge, no experimental vibrational assignment for 2,3DBrNMM (also known as 3,4-dibromo-N-methylpyrrole-2,5-dione) molecule has been performed yet. Also, ab initio Hartree–Fock (HF) and density functional theory (DFT) calculations have not been performed on title

molecule, and analysis of the vibrational modes of this molecule using quantum chemical methods has not been published in the literature so far.

In this study, we recorded FT-IR, FT-Raman, ^{1}H NMR and ^{13}C NMR spectra of title compound and calculated the vibrational frequencies of 2,3DBrNMM in the ground state to distinguish fundamentals from experimental vibrational frequencies and geometric parameters using HF and DFT/B3LYP (Becke 3-Lee-Yang-Parr) methods. In addition, the gauge-including atomic orbital (GIAO) ^{13}C and ^{1}H chemical shifts calculations of the title compound were calculated by using HF and B3LYP methods with 6-311++G(d,p) basis set. A detailed quantum chemical study will aid in making definite assignments to fundamental normal modes of 2,3DBrNMM and in clarifying the experimental data for this important molecule.

## 2. Experimental

The compound 2,3DBrNMM molecule in solid state was purchased from Sigma–Aldrich chemical company with a stated purity of 99%. The FT-IR spectrum of title molecule was recorded between 4000 $cm^{-1}$ and 400 $cm^{-1}$ on a Perkin Elmer FT-IR System Spectrum BX spectrometer which was calibrated using polystyrene bands. The spectrum was recorded at room temperature, with a scanning speed of 10 $cm^{-1}$ $min^{-1}$ and the spectral resolution of 4.0 $cm^{-1}$. FT-Raman spectra of the sample was recorded on a Bruker RFS 100/S FT-Raman instrument using 1064 nm excitation from an Nd:YAG laser. The detector is a liquid nitrogen cooled Ge detector. Five hundred scans were accumulated at 4 $cm^{-1}$ resolution using a laser power of 100 mW.

NMR experiments were performed in Varian Infinity Plus spectrometer at 300 K. The 2,3DBrNMM molecule was dissolved in chloroform ($CDCl_3$). Chemical shifts were reported in ppm relative to tetramethylsilane (TMS) for ^{1}H NMR, ^{13}C NMR and DEPT NMR spectra. ^{1}H and ^{13}C NMR spectra were obtained at a base frequency of 75 MHz for ^{13}C and 300 MHz for ^{1}H nuclei.

## 3. Calculations

The molecular structure of 2,3DBrNMM in the ground state (*in vacuo*) was determined with HF and B3LYP employing the 6-31G(d), 6-31G(d,p), 6-31+G(d,p), 6-31++G(d,p), 6-311G(d), 6-311G(d,p), 6-311+G(d,p) and 6-311++G(d,p) basis sets. The optimized structural parameters are used in the vibrational frequencies calculations at HF and DFT levels. By using the same methods and basis sets, it was seen that all the vibration frequencies of title molecule were positive. Therefore, we were confident that a definite absolute minimum in the potential energy surface was found. The minimum energy of geometrical structure is obtained by using level 6-311++G(d,p) basis set. Therefore, calculated values by this set are used in discussion. The calculated vibrational frequencies are scaled by 0.9050 for HF [12]. For B3LYP with 6-311++G(d,p) basis set, the wavenumbers in the ranges from 4000 to 1700 $cm^{-1}$ and lower than 1700 $cm^{-1}$ are scaled with 0.958 and 0.983, respectively [13]. The total energy distribution (TED) was calculated by using the SQM program [14] and the fundamental vibrational modes were characterized by their TED. The theoretical results have enabled us to make the detailed assignments of the experimental IR and Raman spectra of title molecule.

For NMR calculations, the title molecule was firstly optimized at HF and B3LYP methods with 6-311++G(d,p) level. After optimization, ^{1}H NMR and ^{13}C NMR chemical shifts ($\delta_H$ and $\delta_C$) were calculated using the GIAO method [15] in chloroform ($CDCl_3$) at HF and B3LYP methods with 6-311++G(d,p) basis set. Relative chemical shifts were then estimated by using the corresponding TMS shield-

ing calculated in advance at the same theoretical level as the reference. [13]C and ^{1}H isotropic magnetic shielding (I.M.S.) of any X carbon (or hydrogen) atom was made according to the value ^{13}C IMS of TMS: $CS_x = IMS_{TMS} - IMS_x$ (^{1}H IMS of TMS: $HS_x = IMS_{TMS} - IMS_x$). Calculated ^{1}H and ^{13}C isotropic chemical shieldings for TMS at HF and B3LYP methods with 6-311++G(d,p) level in $CDCl_3$ by using the IEFPCM method were 32.421 ppm, 31.884 ppm and 196.365 ppm, 184.252 ppm, respectively. The experimental values for ^{1}H and ^{13}C isotropic chemical shifts for TMS were 30.84 ppm and 188.1 ppm, respectively [16].

The calculations are performed by using GaussView molecular visualisation program [17] and *GAUSSSIAN 03* program package on the personal computer [18].

## 4. Results and discussion

The present molecule 2,3DBrNMM which the five membered ring had an envelope from retaining the planarity of the C–C=C–C part belongs to $C_s$ point group symmetry. The title molecule consists of 13 atoms, so it has 33 normal vibrational modes which fall into 22 in-plane vibrations of the A′ species and 11 out-plane vibrations of the A″ species. All the 33 fundamental vibrations are active in both IR and Raman. Calculated energies for title molecule, determined by HF and B3LYP/all basis sets are presented in Table 1. As clearly seen from the values given in Table 1, on the calculated energies, there is a little difference between basis sets for 6-311 (or 6-31), use of the basis sets of larger sizes give rise to increases in the differences between the calculated energies of the title molecule. However, when we compared the 6-31 and 6-311 basis sets the difference is large.

The molecular structure and numbering of the atoms of 2,3DBrNMM is shown in Fig. 1. Since the crystal structure of the title compound is not available in the literature till now, the geometric parameters compared with the maleimide [7,8], *N*-phenylmaleimide [10] and 3-benzoylmethyl-2-chloro-*N*-methylmaleimide (3BM2ClNMM) [19] bond lengths and bond angles. The calculated vibrational frequencies are compared with the experimental FT-IR and FT-Raman spectra of title molecule.

### 4.1. Geometrical structure

The first task for a computational work was to determine the optimized geometry of 2,3DBrNMM. Calculations on 2,3DBrNMM have been performed under the restriction of $C_s$ symmetry with the mirror plane perpendicular to the ring. The optimized structure parameters calculated ab initio HF and DFT (B3LYP) with the 6-31++G(d,p) and 6-311++G(d,p) basis sets are listed in Table 2 in accordance with the atom numbering scheme given in Fig. 1.

As discussed in our previous paper [20,21], it is well known that HF methods underestimate bond lengths; DFT method predicts bond lengths which are systematically too long, particularly the

**Table 1**
Calculated energies for 2,3DBrNMM by HF and B3LYP methods

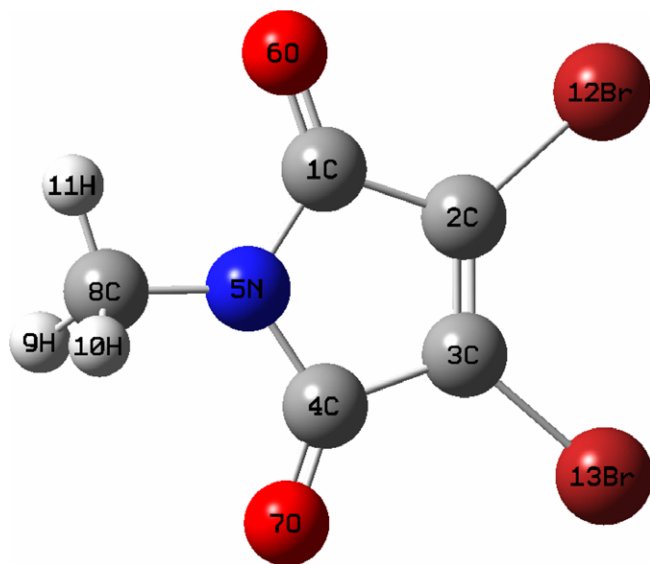| Basis sets | HF | B3LYP |
|---|---|---|
| | Energy (Hartree) | Energy (Hartree) |
| 6-311++G(d,p) | −5540.10192571 | −5545.93978485 |
| 6-311+G(d,p) | −5540.10185337 | −5545.93972968 |
| 6-311G(d,p) | −5540.09486481 | −5545.93082322 |
| 6-311G(d) | −5540.09046665 | −5545.92685895 |
| 6-31++G(d,p) | −5535.10910380 | −5541.01802170 |
| 6-31+G(d,p) | −5535.10886019 | −5541.01781144 |
| 6-31G(d,p) | −5535.05066724 | −5540.94816480 |
| 6-31G(d) | −5535.04587248 | −5540.92685895 |

**Fig. 1.** Optimized geometry of 2,3DBrNMM structure and atoms numbering.

C–H bond lengths. This theoretical pattern also found for title molecule.

The equilibrium structure for the ground state shows that one of the methyl C–H bonds is parallel to the ring plane. The torsional angles C2–C1–N5–C8 and C3–C4–N5–C8 are 179.4 and 179.1 degrees, respectively. The tilt angles are calculated 180 degrees.

The optimized geometry of the maleimide ring part shows very good agreement with experiment. For example, C–N and C=C. The optimized bond lengths of C–N in maleimide ring fall in the range from 1.377 to 1.378 Å for HF/all sets which are in good agreement with experimental values (1.377 and 1.383 Å), seen in Table 2. The same values were calculated for B3LYP/all sets in the range from 1.394 to 1.396 Å. By comparing these values to the experimental ones, it is observed that the B3LYP method overestimate C–N bond lengths. Besides by comparing C=O distances with experimental values of 1.202 and 1.208 Å, as can be seen from Table 2, HF method underestimate and B3LYP overestimate the same.

The optimized bond lengths of C=C in ring are in good agreement with experimental results. For example, C2=C3 is calculated from 1.318 to 1.341 Å. An et al. [19] observed this bond length 1.324 Å. The deviation of atom C8 from the maleimide ring is 1.47 and 1.466 Å for NMM and 3BM2ClNMM, respectively. The N–CH$_3$ bond length is calculated shorter than experimental value for maleimide and 3BM2ClNMM by all the levels.

The C–X (F, Cl, Br, etc.) bond length indicates a considerable increase when substituted in place of C–H. Atom Br is in the plane of the maleimide ring. The C–Br bond length are found 1.864 Å (B3LYP) and 1.853 Å (HF) by using 6-311++G(d,p).

**Table 2**
Optimized geometry of 2,3DBrNMM in the ground state

| Parameters bond lengths (Å) | Exp. [19] 3BM2ClNMM | Exp. [a,b,c] Maleimide, NPM | 6-31++G(d,p) | | 6-311++G(d,p) | |
|---|---|---|---|---|---|---|
| | | | HF | B3LYP | HF | B3LYP |
| C1–C2 | 1.501(4) | 1.508,-,1.489 | 1.508 | 1.510 | 1.511 | 1.513 |
| C1–N5 | 1.383(4) | 1.407,-,1.385 | 1.378 | 1.396 | 1.378 | 1.396 |
| C1–O6 | 1.202(3) | 1.206, -, 1.206 | 1.183 | 1.211 | 1.177 | 1.203 |
| C2–C3 | 1.324(4) | 1.343, 1.34, 1.306 | 1.318 | 1.341 | 1.318 | 1.339 |
| C2–Br12 (Cl) | 1.700(3) | | 1.844 | 1.852 | 1.853 | 1.864 |
| C3–C4 | 1.495(4) | 1.508, 1.48, 1.486 | 1.507 | 1.510 | 1.510 | 1.513 |
| C3–Br13 (Cl) | 1.700(3) | | 1.844 | 1.852 | 1.853 | 1.864 |
| C4–N5 | 1.377(4) | -, -, 1.359 | 1.377 | 1.394 | 1.377 | 1.394 |
| C4–O7 | 1.208(4) | 1.205, 1.22, 1.212 | 1.184 | 1.211 | 1.177 | 1.203 |
| N5–C8 | 1.466(4) | | 1.453 | 1.457 | 1.454 | 1.457 |
| C8–H9 | 0.96 | | 1.082 | 1.093 | 1.082 | 1.091 |
| C8–H10 | 0.96 | | 1.082 | 1.093 | 1.082 | 1.091 |
| C8–H11 | 0.96 | | 1.079 | 1.090 | 1.079 | 1.089 |
| *Bond angles (°)* | | | | | | |
| C2–C1–N5 | 105.5(3) | 106.6, -, 105.5 | 105.82 | 105.86 | 105.79 | 105.73 |
| C2–C1–O6 | 127.8(3) | -, -, 125.4 | 127.30 | 127.87 | 127.24 | 127.88 |
| N5–C1–O6 | 124.7(3) | 124.6, 124, 126.2 | 126.88 | 126.27 | 126.97 | 126.39 |
| C1–C2–C3 | 110.4(3) | -, 110, 109.0 | 108.56 | 108.60 | 108.54 | 108.62 |
| C1–C2–Br12 (Cl) | 120.4(2) | | 121.68 | 121.74 | 121.48 | 121.40 |
| C3–C2–Br12 (Cl) | 129.2(3) | | 129.76 | 129.66 | 129.98 | 129.98 |
| C2–C3–C4 | 106.3(3) | -, -, 108.8 | 108.38 | 108.46 | 108.39 | 108.54 |
| C2–C3–Br13 (Cl) | 129.2(3) | | 129.92 | 129.86 | 130.02 | 129.98 |
| C4–C3–Br13 (Cl) | 120.4(2) | | 121.70 | 121.68 | 121.59 | 121.46 |
| C3–C4–N5 | 107.1(3) | 106.6, 107, 106.0, | 106.00 | 106.01 | 105.95 | 105.84 |
| C3–C4–O7 | 128.0(3) | -, -, 126.2 | 127.61 | 128.10 | 127.56 | 128.10 |
| N5–C4–O7 | 126.5(3) | -, -, 125.4 | 126.39 | 125.89 | 126.48 | 126.06 |
| C1–N5–C4 | 110.6(3) | -, 110, 109.6 | 111.24 | 111.07 | 111.33 | 111.27 |
| C1–N5–C8 | 125.4(3) | | 124.96 | 124.78 | 124.95 | 124.66 |
| C4–N5–C8 | 124.1(3) | | 123.80 | 124.14 | 123.72 | 124.06 |
| N5–C8–H9 | 109.5 | | 110.09 | 110.26 | 110.14 | 110.30 |
| N5–C8–H10 | 109.5 | | 110.09 | 110.26 | 110.14 | 110.30 |
| N5–C8–H11 | 109.5 | | 107.66 | 107.50 | 107.75 | 107.56 |
| H9–C8–H10 | 109.5 | | 109.26 | 109.02 | 109.42 | 109.09 |
| H9–C8–H11 | 109.5 | | 109.86 | 109.89 | 109.69 | 109.79 |
| H10–C8–H11 | 109.5 | | 109.86 | 109.89 | 109.69 | 109.79 |
| C2–C1–N5–C8 | 179.4(3) | | 180.00 | 180.00 | 180.00 | 180.00 |
| C3–C4–N5–C8 | 179.1(3) | | 180.00 | 180.00 | 180.00 | 180.00 |

[a] From Ref. [8].
[b] From Ref. [7].
[c] From Ref. [10].

The maleimide ring is also evident from the negative deviation of C2–C1–N2 and C3–C4–N5 angles which are calculated ca. 105° and 106° (HF and B3LYP) and positive deviation of C1–N5–C4 (111°) angle from the normal value of 108°. The remaining angles are calculated normal value of pentagonal ring. Similar values were obtained for 3BM2ClNMM [19].

## 4.2. Vibrational spectra

In order to obtain the spectroscopic signature of 2,3DBrNMM molecule, we performed a frequency calculation analysis. Calculations were made for a free molecule in vacuum, while experiments were performed for solid sample, so there are disagreements between calculated and observed vibrational wavenumbers.

Experimental and theoretical Raman and Infrared spectra are shown in Figs. 2 and 3, respectively. The experimental wavenumbers are tabulated in Table 3 together with the calculated wavenumbers of studied molecule. The resulting vibrational frequencies for the optimized geometries and the proposed vibrational assignments as well as IR intensities and Raman scattering activities are given in Table 3. All of the calculated modes are numbered from the biggest to the smallest frequency within each fundamental wavenumbers, $vn$, in the first column of the table. In the last column, a detailed description of the normal modes based on the total energy distribution (TED) is given.

For 2,3DBrNMM, group the vibrational modes can be classified, C–H stretching, C=O stretching, C=C stretching, C=N stretching, C–C stretching, C–Br stretching, N–Me stretching, ring stretching, C–C–H bending, C–H bending, C–Br bending, C=O bending, C–C–
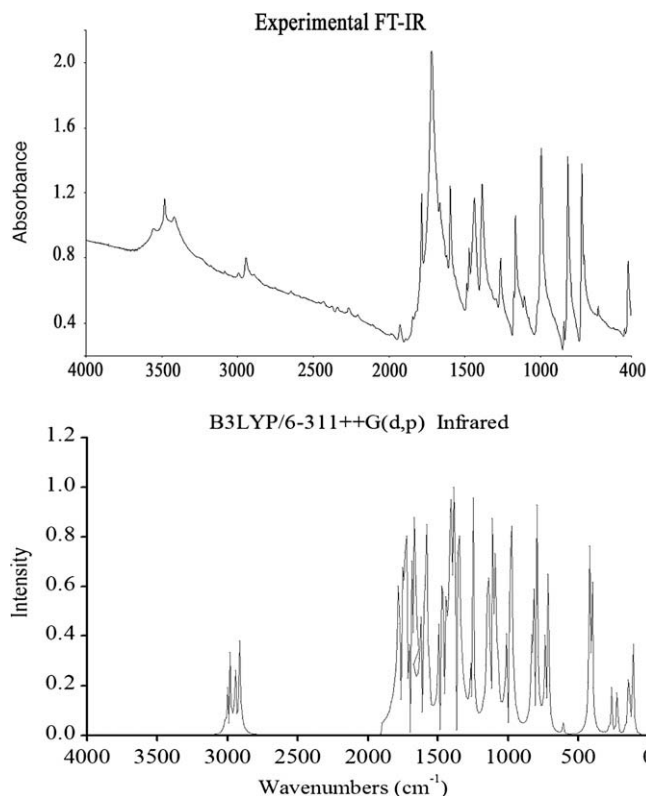


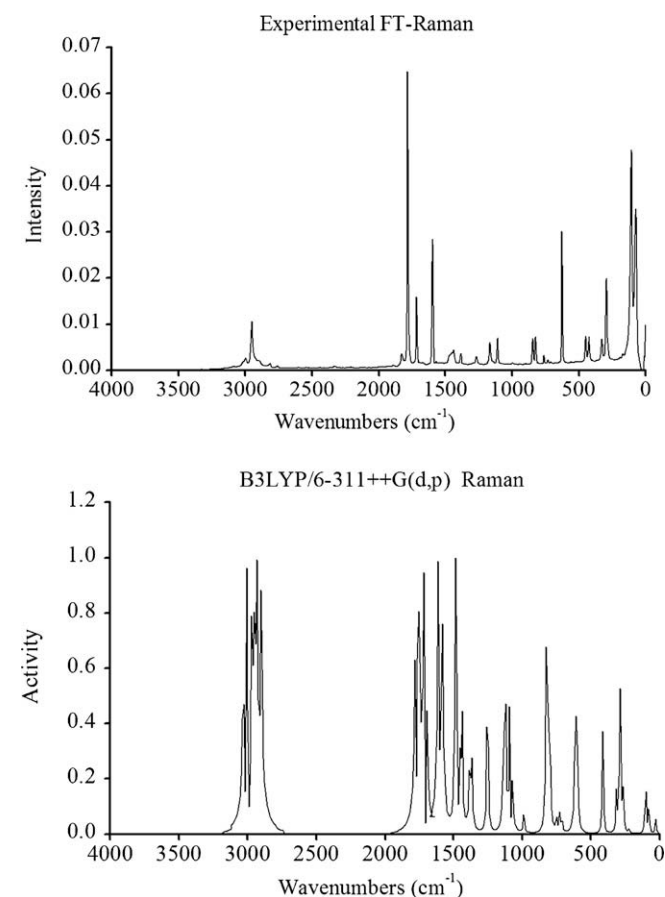Fig. 3. Experimental and theoretical Infrared spectra of 2,3DBrNMM.

C bending, C–C–N bending, C–N–H bending, ring bending, ring breathing, and ring torsion modes.

A major coincidence of theoretical values with that of experimental evaluations is found in the symmetric and asymmetric vibrations of the $CH_3$ moiety ($v1$ and $v3$). The asymmetric stretching for the $NH_2$, $CH_2$ and $CH_3$ has magnitude higher than the symmetric stretching [22]. The symmetric stretching of $CH_3$ is observed in FT-IR at 2945 cm$^{-1}$ (2946 cm$^{-1}$ in FT-Raman) and calculated ($v3$) about at 2901 cm$^{-1}$ at HF level, while DFT estimates it 2924 cm$^{-1}$. The asymmetric stretching of $CH_3$ observed in FT-IR at 2991 cm$^{-1}$ ($v2$) was calculated at 2964 cm$^{-1}$ and 2986 cm$^{-1}$ with HF and B3LYP methods, respectively. The TED of these modes is 100%. Parker [3] assigned these bands at 2930 and 2903 cm$^{-1}$ both FT-IR and FT-Raman for N-methylmaleimide. The mode $v2$ frequency corresponds to the asymmetric stretch of methylene hydrogen atoms of the methyl group. The $CH_3$ bending is observed vibration band near 1450 cm$^{-1}$ [22,23]. In this study, the 1436, 1472 and 1487 cm$^{-1}$ FT-IR (1432 cm$^{-1}$ FT-Raman) bands correspond to internal bending vibrations of the $CH_3$ group. DFT method agrees with the experimental value. These vibrational frequencies calculated (1438–1487 cm$^{-1}$) and assigned as modes $v7$–$v9$. Parker [3] assigned $CH_3$ bending modes as 1440 and 1456 cm$^{-1}$ both for FT-IR and FT-Raman. The $CH_3$ rocking mode is observed at 1150 cm$^{-1}$ for N-Methylmaleimide [3]. The $v15$ mode ($CH_3$ rocking) is observed at 997 cm$^{-1}$ in FT-IR, which is calculated as 989 cm$^{-1}$ by DFT method. The methyl group assignments proposed in this study is also in agreement with the literature values [21,22,24–26].

Raman spectroscopy requires a change in polarisability, thus is more sensitive to the non-polar motions of the molecule while Infrared spectroscopy requires a change in dipole moment thus is sensitive to the polar motions of the molecule. These two techniques provide information on the heavy atom motions of the molecule, for example $vC=C$, $vC=O$ [4]. The very strong bands at



Fig. 2. Experimental and theoretical Raman spectra of 2,3DBrNMM.

**Table 3**
Comparison of the calculated and experimental (FT-IR and FT-Raman) vibrational spectra of 2,3DBrNMM

| Mode No. | Symmetry species | HF/6311++G(d,p)x | | | | B3LYP/6311++G(d,p) | | | | Experimental | | TED[c] (%) |
|---|---|---|---|---|---|---|---|---|---|---|---|---|
| | | Unscaled freq. | Scaled freq.[a] | $I^{Infrared}$ | $S^{Raman}$ | Unscaled freq. | Scaled freq.[b] | $I^{Infrared}$ | $S^{Raman}$ | FT-IR | FT-Raman | |
| | | | | | | | | | | 3484 | | Combination |
| $v1$ | A′ | 3312 | 2997 | 2 | 38.5 | 3153 | 3020 | 0.4 | 39.4 | | | $\nu$CH$_3$(100) asym. |
| $v2$ | A″ | 3275 | 2964 | 19.3 | 62.4 | 3117 | 2986 | 11.5 | 77.1 | 2991 | | $\nu$CH$_3$(100) asym. |
| $v3$ | A′ | 3205 | 2901 | 37.3 | 147.7 | 3052 | 2924 | 30.1 | 193.4 | 2945 | 2946 | $\nu$CH$_3$(100) sym. |
| | | | | | | | | | | 1930 | | Combination |
| $v4$ | A′ | 2055 | 1860 | 90.8 | 96.9 | 1841 | 1764 | 46.9 | 97.8 | 1783 | 1783 | $\nu$C=O(87) sym. |
| $v5$ | A′ | 1958 | 1772 | 1044.9 | 17.6 | 1785 | 1709 | 684.6 | 38.1 | 1717 | 1714 | $\nu$C=O(90) asym. |
| $v6$ | A′ | 1813 | 1641 | 50.9 | 128.7 | 1626 | 1598 | 87.5 | 85.2 | 1595 | 1596 | $\nu$C=C(80) |
| $v7$ | A′ | 1634 | 1479 | 13.4 | 8.7 | 1512 | 1487 | 9.3 | 11 | 1487 | | $\delta$CH$_3$(50) + $\delta$HCN(21) + $\tau$ HCNC(21) |
| $v8$ | A″ | 1608 | 1456 | 10.6 | 9 | 1489 | 1464 | 11.2 | 10.4 | 1472 | | $\delta$CH$_3$(58) + $\tau$HCNC(20) + $\delta$HCN(14) |
| $v9$ | A′ | 1596 | 1445 | 175.6 | 4.6 | 1463 | 1438 | 97.5 | 5.3 | 1436 | 1432 | $\delta$CH$_3$(37) + $\delta$HCN(35) + $\nu$CN(9) ring |
| $v10$ | A′ | 1545 | 1398 | 324 | 1.1 | 1399 | 1375 | 270.7 | 12.2 | 1387 | 1382 | $\nu$CN(45) sym. ring + $\delta$CH$_3$(12) + $\delta$NCO(10) + $\delta$HCN(8) + $\delta$CNC(8) |
| $v11$ | A′ | 1416 | 1281 | 18 | 10.3 | 1276 | 1254 | 19.6 | 6.9 | 1265 | 1260 | $\nu$CN(31) asym. ring + $\delta$HCN(29) + $\tau$HCNC(20) + $\delta$CNC(10) + $\delta$NH(4) |
| $v12$ | A″ | 1296 | 1173 | 89.8 | 6.8 | 1150 | 1131 | 0.3 | 0.8 | 1164 | 1160 | $\delta$HCN(76) ring + $\tau$HCNC(24) |
| $v13$ | A′ | 1252 | 1133 | 1.9 | 1 | 1148 | 1128 | 109.5 | 15 | 1107 | 1108 | $\nu$CC(34) + $\delta$CCC(24)(ring def.) + $\delta$CCBr(16) + $\nu$CBr(11) |
| $v14$ | A′ | 1208 | 1093 | 4.2 | 9.9 | 1103 | 1084 | 16 | 13.5 | 1079 | | $\nu$CC(53) + $\nu$ N-CH$_3$(29) + $\nu$CBr(7) + $\delta$CCO(6) |
| $v15$ | A′ | 1110 | 1004 | 119.9 | 0.6 | 1006 | 989 | 91.1 | 1 | 997 | | $\nu$CN(46) asym. + CH$_3$(31) rock + $\delta$HCN(20) |
| $v16$ | A′ | 904 | 818 | 10.6 | 5.4 | 841 | 826 | 9.7 | 5.9 | 845 | 844 | $\nu$N–CH$_3$(31) + Ring breathing($\nu$CC(17) + $\nu$ CC(16) + $\nu$CBr(21) + $\delta$CCO(3)) |
| $v17$ | A′ | 895 | 810 | 57.1 | 12.5 | 821 | 807 | 55.0 | 14.5 | 821 | 819 | Ring def.($\nu$CBr(29) + $\nu$ CC(21) + $\delta$NCO(14) + $\delta$CCN(9) + $\delta$CCC(7)) |
| $v18$ | A″ | 849 | 768 | 0.2 | 3.4 | 763 | 750 | 0.1 | 0.6 | | 753 | $\gamma$CNCO(34) + $\gamma$OCCBr(24) + $\gamma$CCCN(18) + $\gamma$CCCC(13) |
| $v19$ | A″ | 823 | 745 | 43 | 1 | 738 | 726 | 23.4 | 0.7 | 728 | 720 | $\gamma$CNCC(26) + $\gamma$OCCBr(23) + $\gamma$CNCO(18) + $\gamma$CCCO(12) + $\gamma$CCCN(9) |
| $v20$ | A′ | 785 | 711 | 0.1 | 0.1 | 723 | 710 | 0.3 | 0.4 | 713 | | $\delta$CCO(33) + $\delta$CCBr(25) + $\delta$NCO(22) + $\nu$ CC(7) + $\delta$CNC(6) + CH$_3$(5) rock |
| $v21$ | A′ | 672 | 608 | 0.2 | 10.5 | 619 | 609 | 0.4 | 14.5 | 621 | 624 | $\delta$CCN(22) + $\delta$CNC(21)ring + $\nu$CN(14)ring + $\delta$NCO(13) + $\nu$ CN(9) + $\nu$ NCH$_3$(5) |
| $v22$ | A″ | 503 | 455 | 0 | 0.4 | 454 | 446 | 0 | 0 | 447 | 449 | $\gamma$CCCO(21) + $\gamma$CNCO(16) + $\gamma$CCCBr(4) + $\gamma$CCCC(4) |
| $v23$ | A′ | 459 | 416 | 43.5 | 3.7 | 421 | 413 | 33.9 | 3.8 | 420 | 421 | $\delta$CCO(28) + $\nu$ CN(18) + $\nu$ CBr(15) + $\delta$NCO(13) + $\nu$ N-CH$_3$(10) + $\delta$CNC(7) |
| $v24$ | A′ | 347 | 314 | 0.3 | 2.3 | 319 | 313 | 0 | 1.5 | | 323 | $\nu$CBr(42) + $\delta$CCBr(18) + $\delta$CCC(11) + $\delta$CCO(8) + $\delta$CCN(7) + $\nu$ CC(7) |
| $v25$ | A′ | 318 | 287 | 1.1 | 6.6 | 292 | 287 | 0.2 | 6.4 | | 294 | $\nu$CBr(45) + $\nu$ CC(26) + $\delta$NCO(13) + $\delta$CCO(8) |
| $v26$ | A′ | 297 | 269 | 2.5 | 1.0 | 271 | 259 | 1.9 | 1.4 | | | $\delta$CNCH$_3$(66) (rock CH$_3$) + $\delta$NCO(14) + $\delta$CCO(4) + $\nu$ CBr(3) |
| $v27$ | A″ | 253 | 229 | 4.5 | 0.2 | 228 | 219 | 1.8 | 0.1 | | | $\gamma$CCCBr(29) + $\gamma$NCCBr(25) + $\gamma$OCCBr(15) + $\gamma$CNCC(9) + $\omega$ CH$_3$(5) |
| $v28$ | A′ | 184 | 166 | 0.1 | 0.0 | 169 | 162 | 0.2 | 0.0 | | | $\delta$CCBr(55) + $\nu$ CBr(11) + $\nu$CC(10) + $\delta$CCC(7) + $\delta$NC-CH$_3$(7) |
| $v29$ | A″ | 149 | 134 | 3.9 | 0.0 | 145 | 139 | 3.6 | 0.0 | | | $\gamma$CNCO(34) + $\gamma$HCNC(27) + $\gamma$CCCO(19) + $\gamma$CNCC(13) |
| $v30$ | A″ | 117 | 106 | 5.2 | 0.0 | 114 | 109 | 5.1 | 0.0 | | 107 | $\gamma$NCC-CH$_3$(28) + $\gamma$NCO-CH$_3$(16) + $\gamma$NCCBr(16) + $\omega$ CH$_3$(11) |
| $v31$ | A′ | 115 | 104 | 0.0 | 1.9 | 104 | 99 | 0.1 | 2.3 | | | $\delta$CCBr(94) |
| $v32$ | A″ | 84 | 76 | 0.0 | 0.7 | 78 | 75 | 0.0 | 0.9 | | 71 | $\gamma$CCCBr(20) + $\gamma$NCCBr(14) + $\gamma$CCCO(13) + $\gamma$CCCN(13) + $\gamma$OCCBr(13) |
| $v33$ | A″ | 20 | 18 | 0.1 | 0.3 | 41 | 39 | 0.0 | 0.6 | | | $\tau$CH$_3$(100) |
| $\sigma$ (RMS) | | | 28.374 | | | | 13.122 | | | | | |
| $R^2$ | | | 0.9983 | | | | 0.9997 | | | | | |

$N$, stretching; $\delta$, in-plane bending; $\gamma$, out-of-plane bending; $\rho$, scissoring; $\omega$, wagging; $\tau$, torsion.
[Frequency (cm$^{-1}$), IR intensities; $I^{Infrared}$ (km mol$^{-1}$), Raman scattering activities; $S^{Raman}$ (Å amu$^{-1}$); $R^2$, correlation value].

[a] Scale factor of 0.9050 was used for HF/6-311++G(d,p) basis set [12].
[b] Wavenumbers in the ranges from 4000 to 1700 cm$^{-1}$ and lower than 1700 cm$^{-1}$ are scaled with 0.958 and 0.983 for B3LYP/6-311++G(d,p) basis set, respectively [13].
[c] Total energy distribution (TED).

1717 cm$^{-1}$ in FT-IR (1714 cm$^{-1}$, FT-Raman) and 1783 cm$^{-1}$ in FT-IR (1783 cm$^{-1}$, FT-Raman) spectra were assigned as asymmetric and symmetric C=O stretching vibration, respectively. The theoretically computed values (1764 and 1709 cm$^{-1}$, B3LYP) show very good agreement with experimental results. The HF method calculated $v$(C=O) frequencies higher than the B3LYP method. Lokshin et al. [6] observed C=O symmetric stretching vibration at 1771 cm$^{-1}$ in FT-Raman (1773 cm$^{-1}$, FT-IR solid) and asymmetric stretching vibration at 1724 cm$^{-1}$ in FT-IR. These bands are assigned at 1770, 1712 and 1580 cm$^{-1}$ for maleimide by Harsanyi et al. [7]. Wolbaek [27] observed C=O vibrations at 1775 and 1756 cm$^{-1}$ for maleimide. For N-methylmaleimide, Parker [3] observed C=O vibrations at 1751 and 1701 cm$^{-1}$ in FT-IR (1757 and 1694 cm$^{-1}$, FT-Raman) symmetric and asymmetric stretching, respectively. The C=O symmetric and asymmetric stretching vibrations are assigned at 1775 and 1719 cm$^{-1}$ FT-IR (1766 and 1720 cm$^{-1}$, FT-Raman) and calculated at 1856 and 1805 cm$^{-1}$ for N-phenylmaleimide [4]. The bands at 420 and 713 cm$^{-1}$ in FT–IR (421 cm$^{-1}$ in FT-Raman) spectra are assigned to C=O in-plane bending and the band at 447 cm$^{-1}$ in FT-IR (449 cm$^{-1}$ in FT-Raman) is assigned out-of-plane bending which are supported by calculation also. For N-methylmaleimide, C=O in-plane bending is observed at 695 cm$^{-1}$ solid phase (708 cm$^{-1}$ gases phase) FT-IR [4]. For maleimide, C=O vibrations are assigned at 415 and 778 cm$^{-1}$ in-plane and out-plane bending, respectively [7]. The present calculated modes agree well with the values in the experimental (modes 20, 22–23) [27].

The C=C aromatic stretching vibration predicted at 1598 cm$^{-1}$ ($v$6) is in excellent agreement with experimental observations of both FT-IR (1595 cm$^{-1}$) and FT-Raman (1596 cm$^{-1}$) spectra in Table 3. The C=C aromatic stretch is assigned at 1594 cm$^{-1}$ in FT-IR (1586 cm$^{-1}$, FT-Raman) [6]. Wolbaek [27] observed C=C vibration at 1580 cm$^{-1}$ for maleimide. Parker [4] observed this band at 1586 cm$^{-1}$ in FT-IR (1585 cm$^{-1}$, FT-Raman) for N-phenylmaleimide. The other C–C stretch band is assigned at 1109 cm$^{-1}$ in FT-IR for N-methylmaleimide. We assigned this band at 1107 and 1079 cm$^{-1}$ in FT-IR which is calculated at 1128 and 1084 cm$^{-1}$, respectively in this work. When the ring modes in maleimide are compared to 2,3DBrNMM molecule, which contain one substituent group attached to a ring, it is seen that the ring modes (C=C, C=O, etc.) of maleimide are different in 2,3DBrNMM molecule. This difference seen in the ring modes with the inclusion of a substituent group to maleimide can be explained depending on the corresponding changes in the reduced masses and force constants. The other theoretically calculated C–C–C out-of-plane and in-plane bending modes (ring deformation) have been found to be consistent with the recorded spectral values. The remainder of the observed and calculated frequencies accounted in Table 3, which are in agreement with experimental values in the literature [3,4,6–8].

The C–N stretching frequency is a rather difficult task since there are problems in identifying these frequencies from other vibrations. Gall et al. [28] assigned C–N stretching at 1350 and 936 cm$^{-1}$ for maleimide. For N-methylmaleimide, Parker [3] observed the bands at 1388 and 1254 cm$^{-1}$ in FT-IR and at 1384 and 1254 cm$^{-1}$ in FT-Raman and assigned to C–N symmetric and asymmetric stretching vibrations, respectively. The same vibrations were obtained at 1394 and 1146 cm$^{-1}$ for N-phenylmaleimide [4]. In the present work, the bands assigned at 1387 cm$^{-1}$, 1265 in FT-IR (1382 cm$^{-1}$, 1260 cm$^{-1}$, FT-Raman) and at 997 cm$^{-1}$ in FT-IR spectrum have been assigned to C–N symmetric and asymmetric stretching vibration, respectively. The theoretically computed values of C–N stretching vibration deviate negatively by B3LYP and positively by HF from experimental value. The TED for this mode suggests that this is a mixed mode ($v$10– $v$11, $v$15).

The FT-IR and FT-Raman stretching mode (at 845 and 844 cm$^{-1}$, respectively) corresponding to N–CH$_3$ moiety was calculated at 826 cm$^{-1}$ with B3LYP (unscaled value is 841 cm$^{-1}$, agrees with experiment) in Table 3.

The assignments of C–Br stretching and deformation vibrations have been made on the basis of the calculated TED. Mooney [29,30] assigned vibrations of C–X group (X = Cl, Br, I) in the frequency range of 1129–480 cm$^{-1}$. The C–Br stretching mode appears at longer wavelength region (200–480 cm$^{-1}$) as reported by Varsanyi [31]. In FT-Raman spectrum of 2,3DBrNMM, the band at 294 cm$^{-1}$ is assigned to C–Br stretching vibration coupled with ring deformation (mode $v$25). The theoretical wavenumber of this band (287 cm$^{-1}$) coincides well with the experimental, and the calculated TED (in 45%), confirms this assignment. Moreover, modes $v$17 and $v$13, observed at 821 and 1107 cm$^{-1}$, in infrared spectrum, involve some contribution from the C–Br stretching vibration. The C–Br in-plane bending vibration is assigned at 323 cm$^{-1}$ in FT-Raman, which is calculated at 313 cm$^{-1}$. This is in agreement with the literature data [29–33].

The experimental bands at 3484 cm$^{-1}$ and at 1930 cm$^{-1}$ in FT-IR spectrum do not correspond to a fundamental transition; however, they should be ascribed as the combination bands. The remainder of the observed and calculated frequencies accounted in Table 3.

The infrared intensity for title molecule from experimental fundamentals at 1717 cm$^{-1}$ ($v$5) is very strong, theoretical intensity of these fundamentals is in the same order for HF and B3LYP methods. While experimental intensity is very strong for this mode, calculated intensity is 1044.9 and 684.6 km mol$^{-1}$ for HF and B3LYP methods, respectively (see Table 3). This mode correspond to $v$(C=O) asymmetric stretching ($v$5).

We present RMS ($\sigma$) values to make comparison with experimental data, based on the calculations bottom of Table 3. As seen in Table 3 the vibrational frequencies calculated by means of the B3LYP method are the closest to experimental data. After scaling, the RMS errors between the observed and scaled frequencies of the molecule are found to be 13.122 and 28.374 and the plots are linear with a unit slope and the correlation ($R^2$) values are found to be 0.9983 and 0.9997 for B3LYP and HF methods, respectively.

### 4.3. NMR spectra

The experimental and calculated values for $^{13}$C and $^{1}$H NMR are shown in Table 4. As in Fig. 1, the studied molecule shows three different carbon atoms, which is consistent with the structure on the basis of molecular symmetry. Due to that fact, three peaks are observed in $^{13}$C NMR spectrum. In DEPT spectra two peaks which appear in 164.255 and 129.628 ppm in $^{13}$C spectrum cannot be observed. Therefore, it can be concluded that the two peaks belong to the maleimide ring and does not contain any H bond. $^{1}$H and $^{13}$C chemical shift values (with respect to TMS) have been

**Table 4**
Experimental and theoretical, $^{13}$C and $^{1}$H NMR isotropic chemical shifts (with respect to TMS) of 2,3DBrNMM by HF and DFT (B3LYP) methods

| Atom | Experimental[a] | HF/6-311++G(d,p)[a] | B3LYP/6-311++G(d,p)[a] |
|---|---|---|---|
| C1 | 164.255 | 166.744 | 170.412 |
| C2 | 129.628 | 152.876 | 156.517 |
| C3 | 129.628 | 153.223 | 156.674 |
| C4 | 164.255 | 167.999 | 171.570 |
| C8 | 25.731 | 25.039 | 26.581 |
| H9 | 3.144 | 2.808 | 2.752 |
| H10 | 3.144 | 2.808 | 2.752 |
| H11 | 3.144 | 3.621 | 3.611 |
| $\sigma$ (RMS) | | 11.823 | 13.906 |
| $R^2$ | | 0.9882 | 0.9880 |

[a] All values in ppm; $R^2$, correlation value.

calculated for the optimized structures of the title compound and compared to the experimental chemical shift values. As can be seen in Fig. 1, molecular structure of the title compound includes maleimide ring. This ring include nitrogen atom which shows electronegative property. On the other side, oxygen atom show more electronegative property than bromine atom. Therefore, the chemical shift values of C1, C4 and C2, C3 have been observed at 164.255 ppm (C=O) and 129.628 ppm (=C–Br) and calculated (with respect to TMS) 166.744, 167.999 ppm and 152.876, 153.223 ppm by using HF method and 170.412, 171.570 ppm and 156.517, 156.674 ppm by using B3LYP method (in Table 4). Similarly, other carbon peak (N–CH$_3$) is observed at 25.731 ppm and calculated at 25.039 and 26.581 ppm by using HF and B3LYP methods, respectively. $^1$H NMR spectrum just one type of protons appears at 3.144 ppm as a singlet. This is in accordance with DEPT spectra which also gives just one –CH$_3$ peak, whereas the chemical shift values (with respect to TMS) of 2.808 and 3.621 ppm, 2.752 and 3.611 ppm have been determined by using HF and B3LYP methods, respectively. As can be seen from Table 4, there is a good agreement between experimental and theoretical chemical shift results for the title compound.

We present RMS ($\sigma$) values to make comparison with experimental data, based on the calculations bottom of Table 4. As seen in Table 4 the NMR isotropic chemical shifts calculated by means of the HF method are the closest to experimental data. The RMS errors between the observed and calculated isotropic chemical shifts of the molecule are found to be 11.823 and 13.906 and the plots are linear with a unit slope and the correlation ($R^2$) values are found to be 0.9882 and 0.9880 for HF and B3LYP methods, respectively.

## 5. Conclusion

In the present work, we have performed the experimental and theoretical vibrational, $^1$H and $^{13}$C chemical shifts analysis of 2,3DBrNMM, for the first time. The molecular geometry, vibrational frequencies, infrared intensities and Raman scattering activities of the molecule in the ground state have been calculated by using ab initio HF and DFT (B3LYP) methods with 6-31G(d), 6-31G(d,p), 6-31+G(d,p), 6-31++G(d,p), 6-311G(d), 6-311G(d,p), 6-311+G(d,p), and 6-311++G(d,p) basis sets. The vibrational frequencies were calculated and scaled values (6-311++G(d,p) basis set) have been compared with experimental FT-IR and FT-Raman spectra. The results calculated by density functional B3LYP and ab initio HF methods indicate that B3LYP is superior to the scaled HF approach for molecular vibrational problems. Similarly, $^1$H and $^{13}$C chemical shifts were calculated by HF and B3LYP methods with 6-311++G(d,p) basis set and were compared with experimental values. The observed and the calculated frequencies and isotropic chemical shifts are found to be in good agreement.

## Acknowledgements

## Appendix A. Supplementary data

Supplementary figures which are related with NMR spectra with this article can be found, in the online version. And the internal coordinates and Gaussian output file are available from the authors, on request. Supplementary data associated with this article can be found, in the online version, at doi:10.1016/j.molstruc. 2008.05.014.

## References

[1] G.T. Gam, J.G. Jeong, N.J. Lee, C.S. Ha, W.J. Cho, J. Appl. Polymer Sci., 57 (1995) 219.
[2] J.P. Cox, F.S. Parker, Acta Cryst. C52 (1996) 2578.
[3] S.F. Parker, Spectrochimica Acta A 51 (1995) 2067.
[4] S.F. Parker, Spectrochimica Acta A 63 (2006) 544.
[5] B.A. Rozenberg, G.N. Boiko, R.J. Morgan, E.E. Shin, Polym. Sci. Ser. A 43 (2001) 386.
[6] B.V. Lokshin, V.T. Aleksanyan, Z.S. Klemenkova, L.V. Rybin, N.T. Gubbnko, J. Organomet. Chem. 74 (1974) 97.
[7] L. Harsányi, P. Császár, G. Fogarasi, G. Horváth, I. Szilágyi, J. Mol. Struct. 104 (1983) 79.
[8] L. Harsányi, É. Vajda, I. Hargittai, J. Mol. Struct. 129 (1985) 315.
[9] D.H.A. ter Steege, W.J. Buma, J. Chem. Phys. 118 (24) (2003).
[10] C.W. Miller, C.E. Hoyle, E.J. Valente, D.H. Magers, E.S. Jönsson, J. Phys. Chem. A 103 (1999) 6406.
[11] C.A. McPhallen, M.N.G. James, Acta Cryst. C39 (1983) 1439.
[12] D.C. Young, Computational Chemistry: A Practical Guide for Applying Techniques to Real World Problems (Electronic), John Wiley & Sons Inc., New York, 2001.
[13] N. Sundaraganesan, S. Ilakiamani, H. Saleem, P.M. Wojciechowski, D. Michalska, Spectrochimica Acta A 61 (2005) 2995.
[14] J. Baker, A.A. Jarzecki, P. Pulay, J. Phys. Chem. A 102 (1998) 1412.
[15] K. Wolinski, J.F. Hinton, P. Pulay, J. Am. Chem. Soc. 112 (1990) 8251.
[16] J.R. Cheeseman, G.W. Trucks, T.A. Keith, M.J. Frisch, J. Chem. Phys. 104 (1996) 5497.
[17] A. Frisch, A.B. Nielsen, A.J. Holder, Gaussview Users Manual, Gaussian Inc., Pittsburg.
[18] M. J. Frisch et al., Gaussian 03, Revision B.4, Gaussian Inc., Pittsburgh PA, 2003.
[19] Hui-Ying An, Zhi-Feng Lu, Yong-Miao Shen, Jian-Hua Xu, Acta Cryst. E62 (2006) o70.
[20] M. Karabacak, M. Çınar, M. Kurt, J. Mol. Struct. 885 (1-3) (2008) 28.
[21] M. Kurt, M. Yurdakul, Ş. Yurdakul, J. Mol. Struct. (Theochem) 711 (2004) 25.
[22] D. Lin-Vien, N.B. Colthup, W.G. Fateley, J.G. Grasselli, The Handbook of Infrared and Raman Characteristic Frequencies of Organic Molecules, Academic Press, 1991.
[23] A.B. Dempster, D.B. Powell, N. Sheppard, Spectrochimica Acta 28A (1972) 373.
[24] M. Silverstein, G. Clayton Basseler, C. Morill, Spectrometric Identification of Organic Compounds, Wiley, New York, 1981.
[25] M. Karabacak, E. Sahin, M. Çınar, İ. Erol, M. Kurt, J. Mol. Struct. 892 (2008) 25.
[26] M. Karabacak, D. Karagöz, M. Kurt, J. Mol. Struct. 892 (2008) 25.
[27] T. Wolbaek, P. Klaboe, C.J. Nielsen, J. Mol. Struct. 27 (1975) 283.
[28] L. Le Gall, P. Caillet, M.T. Forel, J. Chim. Phys. 75 (1978) 444.
[29] E.F. Mooney, Spectrochimica Acta 20 (1964) 1021.
[30] E.F. Monney, Spectrochimica Acta 19 (1963) 877.
[31] G. Varsanyi, Assignments of Vibrational Spectra of 700 Benzene Derivatives, Wiley, New York, 1974.
[32] N. Sundaraganesan, H. Saleem, S. Mohan, M. Ramalingam, V. Sethuraman, Spectrochimica Acta A 62 (2005) 740.
[33] N. Sundaraganesan, C. Meganathan, B. Anand, C. Lapouge, Spectrochimica Acta A 66 (2007) 773.